Dynamic Diagnostics of Limiting State of Milling Process Based on Poincaré Stroboscopic Mapping

A. A. Gubanova

Abstract The article is devoted to the problem of diagnosing the limiting state of the milling process based on the Poincaré stroboscopic mapping. A method based on a contactless measurement of the distance between the cutter body and the measuring transducer is proposed. In this case, a sequence constructed on the basis of the Poincaré stroboscopic mapping is used, for which statistical estimates to determine the roughness, ripple, and mathematical expectation of the size over the entire treated surface are given. The results of the experiment made it possible to obtain effective algorithms for processing information, which, in the course of cutting, allow us to evaluate the limiting states of the process for obtaining information on the replacement of the tool and its readjustment. The dependencies obtained in the work as a whole coincides with the realistic approach to the estimation of the dynamics of milling processes occurring in metal-cutting machines. According to this approach, it is possible to provide unchanged values of the microroughness height due to the redistribution of the geometric component of the roughness determined by the feed, and the evolutionary component that depends on the trajectory of work and the power of irreversible transformations in the cutting zone.

Keywords Surface quality · Milling · Waviness · Roughness · Critical value

1 Introduction

Modern measuring equipment and sensors make it possible to obtain a qualitative idea of the results of the quality of the treated surface on metal-cutting machines in the course of metalworking, in particular when milling. The complexity of studying the dynamics of milling lies in the fact that in the mathematical description of this process, it is necessary to consider nonlinear equations with periodically changing

A. A. Gubanova (✉)
Don State Technical University, 1, Gagarin Square, Rostov-on-Don 344000, Russia
e-mail: Anatoliya81@mail.ru

A. A. Radionov et al. (eds.), *Proceedings of the 4th International Conference on Industrial Engineering*, Lecture Notes in Mechanical Engineering,
https://doi.org/10.1007/978-3-319-95630-5_10

coefficients, which are caused by the intermittence of the cutting process by each tooth of the milling cutter. In this case, the vibrations always accompanying milling have a complex structure, for example, in the vicinity of a stationary periodic trajectory, various attractive sets (limit cycles, invariant tori, and chaotic attractors) can be formed [1]. They have a fairly complex and ambiguous effect on the surface relief being formed. To study the vibrational structure of the observed sequences, it is suggested to use time sequences composed of Poincaré stroboscopic mappings. In the article, it is proved that the mathematical expectation from such sequences allow to identify the stationary trajectories of elastic deformation displacements of the tool relative to the workpiece being machined [2–4].

2 Analysis of the Problem and Formulation of the Research Task

When milling, as well as any processing, due to the energy released in the cutting zone, there are changes in the state of the cutting process and the quality parameters of the parts [5, 6]. First of all, the following parameters are changed: the wear rate of the tool and its wear, the micro- and macro-relief parameters of the surface, and the accuracy characteristics. For a more detailed assessment of changing quality parameters, the following provisions can be used (Fig. 1).

Fig. 1a shows the development of the surface. It identifies cutting and cutting insertion areas from the cutting zone (yellow areas), as well as stationary areas (red color). The direction of movement of the cutting area is indicated by a red arrow. Figure 1b shows the scheme of measurement, and in Fig. 1c, is a gap formation scheme $\Delta(t)$ when the tool is installed with an eccentricity (red curve), the total value of the gap variation that is added from the radial run out of its rotation center and elastic deformation displacements is shown in a blue curve. The development of wear occurs along each cutting blade unevenly. The wear rate is maximum at the points of insertion and the exit of the tool from the cutting zone [7]. We confine ourselves to estimating wear on the back edge in the middle part of the tool, for which we will further illustrate the methodology for estimating the topology of the surface [8]. For a more detailed estimation of the topology, it is convenient to consider spatial (by rotation angle) and (or) time sequences as the initial information (Fig. 1).

The deformation shifts are determined by the steady trajectory. This is the case when the beats are absent, and the stationary trajectory is stable. Then in the phase plane we have a Poincaré stroboscopic map in the form of a point (Fig. 2a). The radial beating of the tool is applied on the deformation of the instrument [9]. In this case, we have a two-frequency trajectory. The trajectory of periodic elastic deformation displacements is a multiple of the beat periods. Then, in the phase plane, we have m points, where m is the coefficient of period multiplicity. Figure 2b shows an example of mappings for a three-tooth mill. In the neighborhood of a stationary

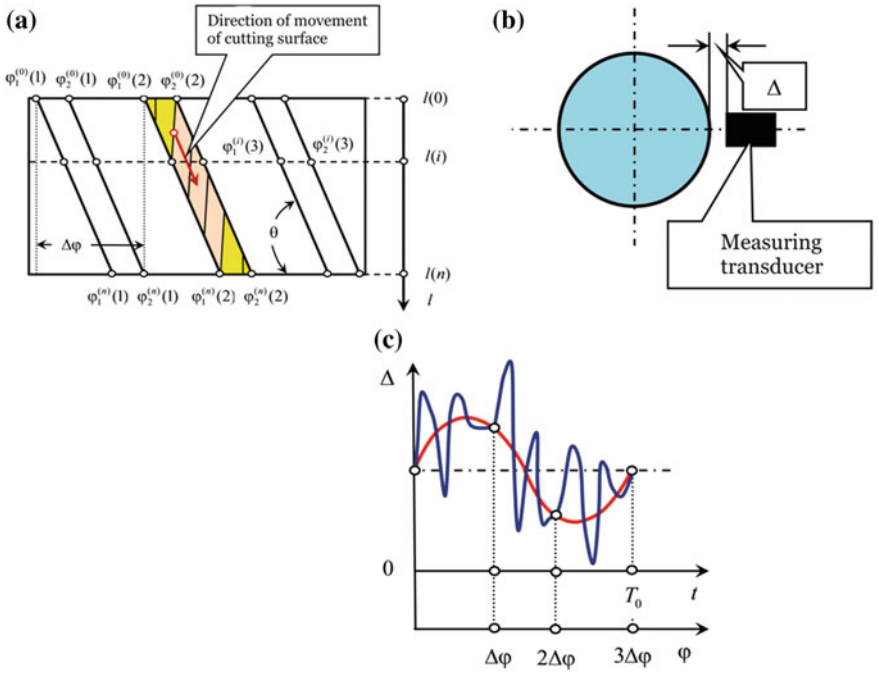

Fig. 1 Scheme for assessing the quality of the surface to be formed on the basis of a noncontact change in the gap between the shank of the mill and the measuring transducer

trajectory, it is possible to form attracting sets in the form of a limit cycle. Then, we have an overlap of three periodic motions. An example of a Poincaré stroboscopic mapping for this case is shown in Fig. 2c. In the vicinity of a stationary trajectory, the formation of a chaotic attractor is possible. In this case, we have a map in the phase plane, an example of which is shown in Fig. 2c. Sequences constructed on the basis of a Poincaré stroboscopic map are easily measurable.

3 Carrying Out the Experiment and Its Results

To diagnose the attainment of the limit set, it is sufficient to ensure observation of a vector $\Delta^{(t)}$ with a period T. Here, is an example of changing the mappings when milling bars—steel 40XH2MA. The width of the bars is 30 mm, the length at which the measurement is made is 100 mm. In addition, to create a surface area in relation to which the relief is measured—20 mm. This is the main area of the surface. Thus, the total length is 120 mm. The tool is from P9K5. The diameter of the milling cutter is 30.0 mm, the number of teeth is 3; the length of the cutting part of the mill is 102 mm. The angle of the teeth is 35°. The arrangement of the teeth is

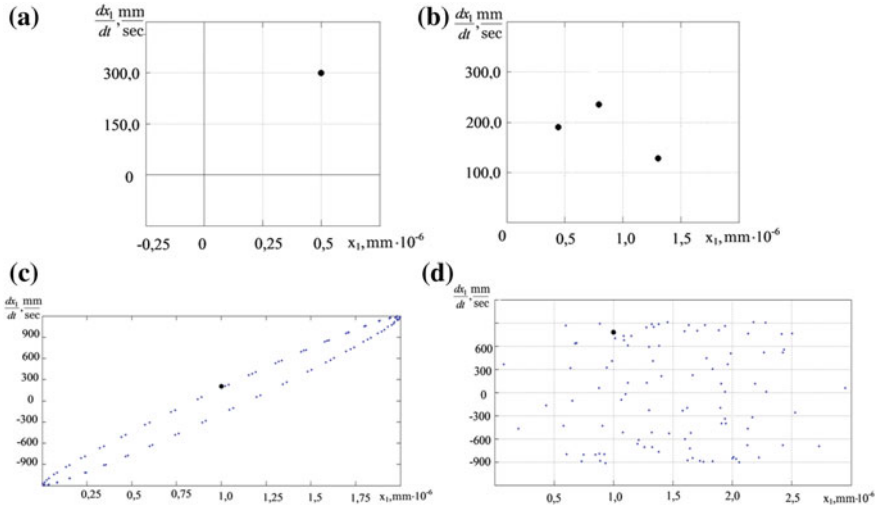

Fig. 2 Examples of sequences constructed using Poincare's stroboscopic mapping algorithms. The periodic component T_q corresponds to the fatty point

symmetrical. Acceptable variations in diameter ΔD = 0.01 mm (limiting variations in allowance). Measurement of the coordinates of the surface is performed on the measuring device DELTA. Modes: cutting speed—0.9 m/s, which corresponds to the rotational speed of the tool 600 rpm; the amount of feed per tooth is 0.05 mm; depth of cut—5.0 mm. Treatment without coolant. Measurement of the gap is carried out by an eddy current sensor with an error not exceeding 1.0 μm.

Thus, during one pass, the vector $\Delta^{(t)}$ consisted of 600 samples. For each vector, the values of the roughness, ripple, and deviation of the part size from the reference surface were aligned. At least 50 passes were made on each bar. A total of 5 bars were processed. All measurements were made on the middle line along the width of the processed bar, that is, at a distance of 15 mm from the edge. Figure 3 shows a fragment of the sequence at the initial stage of processing, a change in its mean value (estimates of mathematical expectation) and the central deviation (variance estimates) are constructed as the number of samples k increases. In the above illustration

$$\hat{\Delta}(k) = \frac{1}{k}\sum_{k=1}^{k=30}\{\Delta(k)\}, \quad \sigma_{\Delta}(k) = \left\{\sum_{k=1}^{k=30}[\Delta(k) - \hat{\Delta}(k)]^2\right\}^{0.5}/k\hat{\Delta}$$

Statistical estimates after 15 counts converge to their steady-state values. To estimate the topology of the surface, we take into account that it is formed as a result of superposition of three additive processes. The first process is related to the given trajectories of the shaping motions taking into account the kinematic trajectory and the established elastic deformations. Therefore, the geometry of the tool

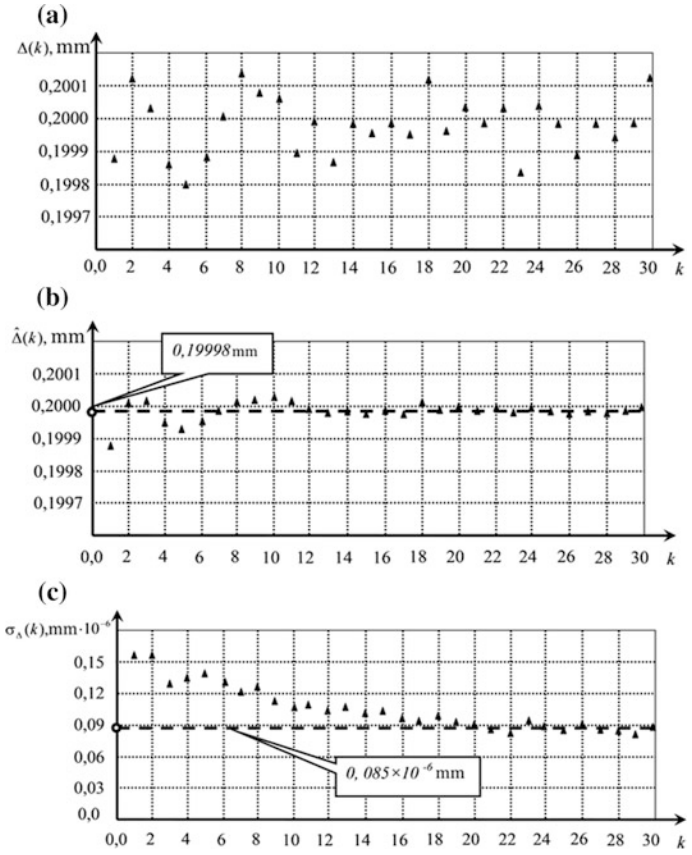

Fig. 3 Fragment of the sequence obtained on the basis of the Poincare stroboscopic map: **a** the initial sequence, **b** mathematical expectation, **c** the relative standard deviation

is actually copied on the surface. The second is related to the features of the dynamics of milling. Dynamic features cause variation of the shaping trajectories. When assessing the microrelief, ripple, and deviation of the shape, various statistical estimates are used, differing in the level of averaging of variations in the topology of the surface. Therefore, we will use the moving average algorithms in different averaging windows. At the same time, estimates should be statistically significant [10–12]. We will consider the following:

The first level is determined by the amount Δk that is dictated by the requirement of obtaining statistical significance. In our case, $\Delta k = 15$ (Fig. 3). In this connection, we can propose the following estimate of the geometry:

$$\hat{\Delta}(s) = \frac{1}{\Delta k} \sum_{i=s}^{i=s+\Delta k} \Delta(i), \quad s = 1, 2, 3\ldots, (s - \Delta k) \tag{1}$$

where $\hat{\Delta}(s) = \left\{\hat{\Delta}(1), \hat{\Delta}(2), \ldots, \hat{\Delta}(s - \Delta k)\right\}^{\mathrm{T}}$—vector of the moving average in a window Δk. This is an estimate of the size change in the direction normal to the surface being formed. For estimating the microrelief, it is convenient to consider the sliding mean square deviation from the mathematical expectation in the window [13], that is

$$\hat{\sigma}_{\Delta}(s) = \left\{ \sum_{i=s}^{i=s+\Delta k} \left[\Delta(i) - \hat{\Delta}s\right]^2 / \Delta k \right\}^{0.5} = 1, 2, 3\ldots(s - \Delta k) \tag{2}$$

where $\hat{\sigma}_{\Delta}(s) = \left\{\hat{\sigma}_{\Delta}(1), \hat{\sigma}_{\Delta}(2), \ldots, \hat{\sigma}_{\Delta}(s - \Delta k)\right\}^{T}$—vector of the moving average variance in the window Δk.

It is known that the estimate of the ripple is different from the roughness by the large averaging step $\Delta k^{(B)}$. In our case, $\Delta k^{(B)} = 50\Delta k$. Therefore, to estimate the ripple, we can use

$$\hat{\sigma}_{\Delta}^{B}(s) = \left\{ \sum_{i=s}^{i=s+\Delta k^{(B)}} \left[\Delta(i) - \hat{\Delta}s\right]^2 \right\}^{0.5} / \Delta k^{(B)} = 1, 2, 3\ldots\left(s - \Delta k^{(B)}\right) \tag{3}$$

The total number of samples k throughout the ensemble can be divided into l subbands by the rule $k = l \cdot p$ (here, p is the length of each subband). In our case, the total length of the treated surface is 5000 mm (100 mm per surface), which corresponds to 30,000 counts (600 samples per surface). Obviously, the general requirement $\Delta k < \Delta k^{(B)} < p$ must be met. In our case, $\Delta k = 15$, $p = 600$ and $l = 50$. Then, the average value of the deviation of the size on each surface from the zero value is determined by

$$\hat{\Delta}_p(l) = \frac{1}{p} \sum_{i=p(l-1)}^{i=pl} \Delta(i) \tag{4}$$

where $\hat{\Delta}_p(l) = \left\{\hat{\Delta}_p(1), \hat{\Delta}_p(2), \ldots, \hat{\Delta}_p(l)\right\}^{T}$—the vector of estimating of the mathematical expectation of deviation of size after each pass. For example, for $l = 5$, the averaging is carried out according to counts (2400–3000). Figure 4 shows an example of an evolutionary trajectory and the corresponding values of the vectors (1, 2). Despite the large data sets, their processing is not difficult since the observed sequences are transmitted through the analog–digital converter (ADC) E14-440 into the computer memory. The permissible sampling frequency in the converter is 100 kHz.

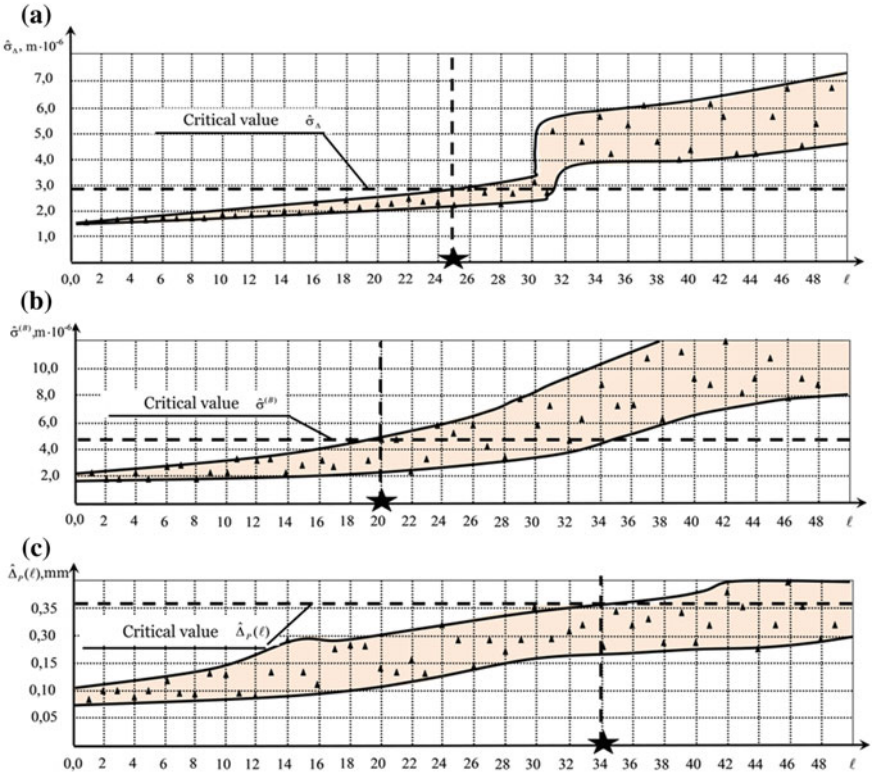

Fig. 4 Evolution of estimates of the Poincaré stroboscopic map

Let us analyze the given data.

- As the number of treated surfaces increases, all the sequence estimates, indicating a monotonous change in size, roughness, and ripple, are shifted. Moreover, with their displacement, the dispersion also increases. Qualitatively, the evolution of estimates is similar.
- With a general tendency to increase all estimates, the dispersion value increases non-monotonically. Estimation of the dynamics of the system shows that the point corresponding to a sharp increase in dispersion $\hat{\sigma}_\Delta$, the system loses its stability and self-oscillations develop in it. It is characteristic that in other assessments, there are no abrupt changes.
- At $l \in (0.4)$ (at the initial stage of processing), the dispersion of the estimates is small. Here, the relief is mainly formed due to the geometric trace from the instrument. On the diagrams of the evolutionary changes in estimates of the Poincaré stroboscopic map, these values correspond to critical estimates, indicated by dashed lines (Fig. 4). It is important to emphasize that they correspond

to different values of the number of treated surfaces. This confirms the importance of diagnosing the marginal set in the processing for making instrument changes.

The estimates in Fig. 4 actually characterize the space for parameter diagnostics: roughness estimate R_a (μm), wave height W_a (μm), and dimensional deviation Δh (mm).

4 Discussion of Results

An analysis of these experimental results and methods of their processing allows us to make two important conclusions. First, the evolution of parameters that evaluate the topology of the surface is interrelated [14–19]. This is natural since the parameters of the microrelief, waviness, and surface shape characterize different estimates of the same process. Therefore, to estimate the attainment of the limit set, one can confine oneself to one of the estimates. Secondly, in the course of evolution of the particular example of a limiting set, estimates of various parameters are not achieved simultaneously. In our case, the microrelief estimate first reaches its limiting value [20]. Therefore, in determining the timing of the changeover and the replacement of the tool, it is sufficient to ensure that the evaluation $\hat{\sigma}_\Delta$ is monitored. Third, when considering, for example, roughness, it is necessary to take into account that the microroughness value is composed of the kinematic component determined by the trace from the tool on the workpiece. It depends on the amount of feed per tooth. It monotonically increases during the evolution of the cutting system during the functioning of the system.

Acknowledgements I express my gratitude to my scientific supervisor Zakovorotniy Vilor Lavrentievich for valuable advice in the planning of research and recommendations on the design of the article.

References

1. Zakovorotny VL, Gubanova AA, Lukyanov AD (2017) Attractive manifolds in end milling. Russ Eng Res 37(2):158–163
2. Goldberg S (1967) Henri Poincaré and Einstein's Theory of Relativity. Am J Phys 35: 934–944
3. Hintikka J (2012) IF logic, definitions and the vicious circle principle. J Philos Logic 41 (2):505–517
4. Budak E, Altintas Y (1995) Modeling and avoidance of static form errors in peripheral milling of plates. J. Mach Tools Manuf 35(3):459–476
5. Tsai JS, Liao CL (1999) Finite-element modelling of static surface errors in the peripheral milling of thin-walled workpiece. J. Mater Process Technol 94:235–246
6. Paris H, Peigne G, Mayer R (2004) Surface shape prediction in high-speed milling. J Mach Tools Manuf 44(15):1567–1576

7. Kersting P, Biermann D (2009) Simulation concept for predicting workpiece vibrations in five-axis milling. J. Mach Sci Technol 13(2):196–209
8. Voronov S, Kiselev I (2011) Dynamics of flexible detail milling. J Multi-body Dyn 225 (3):110–117
9. Lamikiz A, Lopez de Lacalle LN, Sanchez JA, Bravo U (2005) Calculation of the specific cutting coefficients and geometrical aspects in sculptured surface machining. J. Mach Sci Technol 9(3):411–436
10. Surmann T, Enk D (2007) Simulation of milling tool vibration trajectories along changing engagement conditions. J. Mach Tools Manuf 47(9):1442–1448
11. Guzel BU, Lazoglu I (2003) Sculpture surface machining: a generalized model of ball-end milling force system. J. Mach Tools Manuf 43(5):453–462
12. Charpentier E, Ghys E, Lesne A (2010) The scientific legacy of Poincaré. Providence, American Mathematical Society, London Mathematical Society, London, RI
13. Goodman N (1969) Languages of art. An approach to a theory of symbols. Oxford University Press, London
14. Mette C (1986) Invariantentheorie als Grundlage des Konventionalismus. Überlegungen zur Wissenschaftstheorie Jules Henri Poincarés, Die blaue Eule, Essen
15. Zahar E (2001) Poincaré's philosophy.From conventionalism to phenomenology. Open Court, LaSalle
16. Browder FE (1983) The mathematical heritage of Henri Poincaré. In: Proceedings of symposia in pure mathematics of the american mathematical society, vol 39. American Mathematical Society, Providence
17. Darrigol O (2004) The mystery of the Einstein-Poincaré connection. Isis 95:614–626
18. Goldfarb W (1985) Poincaré against the Logicists, in History and Philosophy of Modern Mathematics. In: Aspray W, Kitcher P (eds). Minnesota Press, Minneapolis, pp 61–81
19. Gray JJ (1991) Did Poincaré say set theory is a disease? Math Intell 13(1):19–22
20. Vapnik VN, Chervonenkis AY (1974) Theory of pattern recognition. Nauka, Moscow, pp 55–60. (in Russia)